# SFN #370 28-40
# 担当：小道 雄斗（東大相川研M2）

28 Hydrocarbon chemistry in inner regions of planet forming disks

29 A survey of SiO $J = 1 - 0$ emission toward massive star-forming regions

30 3D structure of HII regions in the star-forming complex S254-S258

31 3D Global Simulations of Accretion onto Gap-opening Planets: Implications for Circumplanetary Disc Structures and Accretion Rates

32 A low-mass line-rich core found in Massive Star-forming Region IRAS 16351-4722

33 A JWST survey of the Trapezium Cluster & inner Orion Nebula. I. Observations & overview

34 Early phases of star formation: testing chemical tools

35 An improved dynamical Poisson equation solver for self-gravity

36 Co-Evolution of Stars and Gas: Using Analysis of Synthetic Observations to Investigate the Star-Gas Correlation in STARFORGE

37 A kinematic study of the disc-outflow system around a high-mass protostar G59.783+0.065 probed by methanol and water masers

38 Early Planet Formation in Embedded Disks (eDisk) X: Compact Disks, Extended Infall, and a Fossil Outburst in the Class I Oph IRS43 Binary

39 Variations of the HCO+, HCN, HNC, $N_2H^+$ and $NH_3$ deuterium fractionation in high-mass star-forming regions

40 Jupiter Mass Binary Objects in the Trapezium Cluster

## 29. A survey of SiO $J = 1 - 0$ emission toward massive star-forming regions

W. -J. Kim, J. S. Urquhart, V. S. Veena, G. A. Fuller, P. Schilke, K-T Kim ★ The application of silicon monoxide (SiO) as a shock tracer arises from its propensity to occur in the gas phase as a result of shock-induced phenomena, including outflow activity and interactions between molecular clouds and expanding HII regions or supernova remnants. We searched for indications of shocks toward 366 massive star-forming regions by observing the ground rotational transition of SiO ($v = 0$, $J = 1 - 0$) at 43 GHz with the Korean VLBI Network (KVN) 21 m telescopes to extend our understanding on the origins of SiO in star-forming regions. We detected SiO emission toward 104 regions that consist of 57 IRDCs, 21 HMPOs, and 26 UCHIIs. The determined median SiO column density, $N$(SiO), and abundance, $X$(SiO), relative to $N(H_2)$ are $8.12 \times 10^{12}$ cm$^{-2}$ and $1.28 \times 10^{-10}$, respectively. These values are similar to those obtained toward other star-forming regions and also consistent with predicted values from shock models with low-velocity shocks ($\lesssim$10 - 15 km s$^{-1}$). While the $X$(SiO) does not exhibit any strong correlation with the evolutionary stages of their host clumps, $L_{SiO}$ is highly correlated with dust clump mass, and $L_{SiO}/L_{bol}$ also has a strong negative correlation with $T_{dust}$. This shows that colder and younger clumps have high $L_{SiO}/L_{bol}$ suggestive of an evolutionary trend. This trend is not due to excess emission at higher velocities, such as SiO wing features, as the colder sources with high $L_{SiO}/L_{bol}$ ratios lack wing features. Comparing SiO emission with $H_2O$ and Class I $CH_3OH$ masers, we find a significant correlation between $L_{SiO}/L_{bol}$ and $L_{CH_3OH}/L_{bol}$ ratios, whereas no similar correlation is seen for the $H_2O$ maser emission. This suggests a similar origin for the SiO and Class I $CH_3OH$ emission in these sources.

複数の大質量星領域でSiO輝線を観測し、統計的に解析

- SiO存在度はおよそ1e-10程度で、進化段階にはあまり依らない。
- SiO輝線はクランプの質量に比例し、ダスト温度が低いほど強い傾向にある。
- SiO輝線強度は$H_2O$メーザー輝線とは相関がそこまで強くない。
  $CH_3OH$メーザーとは相関する。
- 低速度の衝撃波に付随していると思われるSiO輝線が見られた。

# イントロ・観測

- SiO輝線は衝撃波の良いトレーサー。out flowやjetの観測によく用いられる。
- 近年は、星形成領域(更には希薄な分子ガス雲でも)SiO輝線が観測されている。
  空間的にも広く分布しており、必ずしもout flowなどとは付随しない。
- 空間的に広がったSiO輝線の線幅は細く、遅い衝撃波(5-15 km/s)に起因すると
  考えられている。
- 一方で、大質量形成の理解には周辺環境との相互作用(e.g., ガス降着)の
  理解が重要。→ SiO輝線の観測から星形成活動の理解を目指す。

- 観測対象: 計366天体
  134のinfrared dark cloudコア(IRDCs)
  129のhigh-mass protostellar objects (HMPO)
  103の、ultra-compact HII領域(UCHII)を含むクランプ
- 観測: Korean VLBI NetworkによるSiO (1-0) 輝線の観測
- $H_2O$, $CH_3OH$のメーザー輝線のデータとも比較

| Telescope | Beam size (″) | Beam efficiency |
|---|---|---|
| KVN−Yonsei | 61.5 | 0.45 |
| KVN−Ulsan | 61.6 | 0.42 |
| KVN−Tamna | 62.1 | 0.48 |

# 結果

- 106の天体でSiO輝線を検出
  IRDCs: 59, HMPO: 21, UCHII: 26
- 輝線スペクトルをガウシアンでfitting
- SiO検出の有無と物理量の違い

SiOは比較的質量の大きく、
ダスト温度の低い領域で検出されている。

$L_{\rm bol}/M_{\rm clump}$(進化の指標)の低い(進化が進んでいない)
領域で検出される傾向にある。

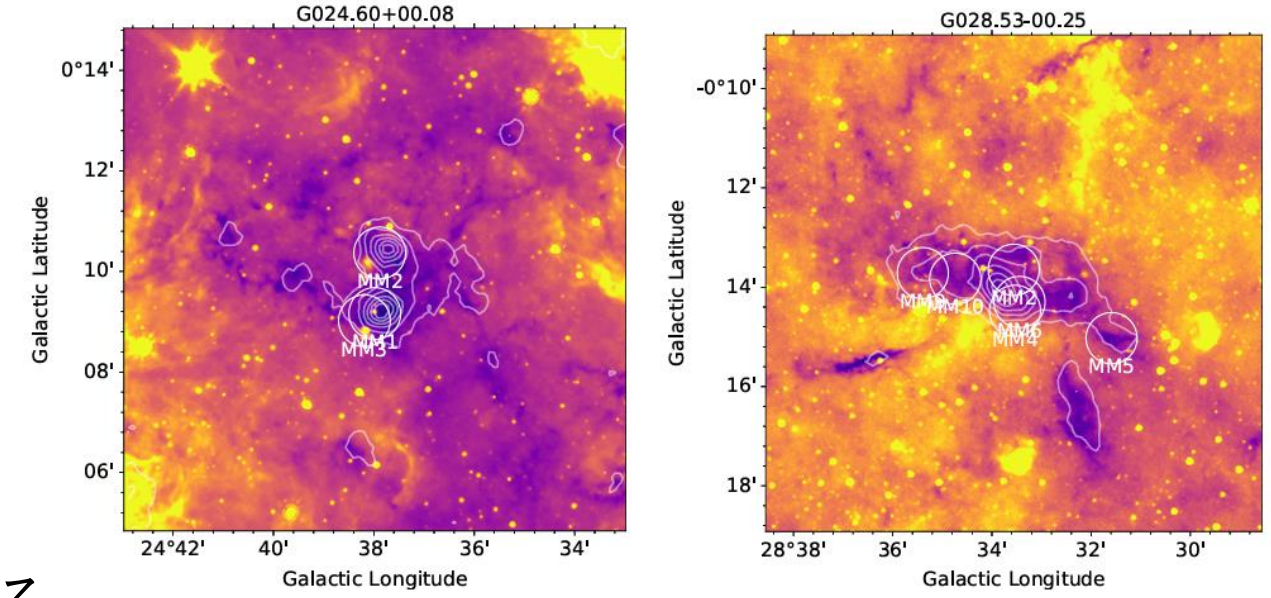


color: 8 μm, gray contours: 870 μm
white circle: beam of KVN

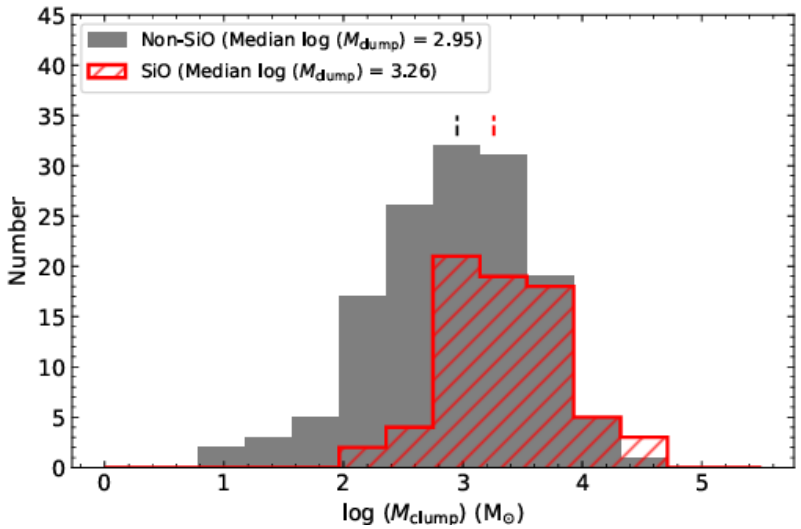


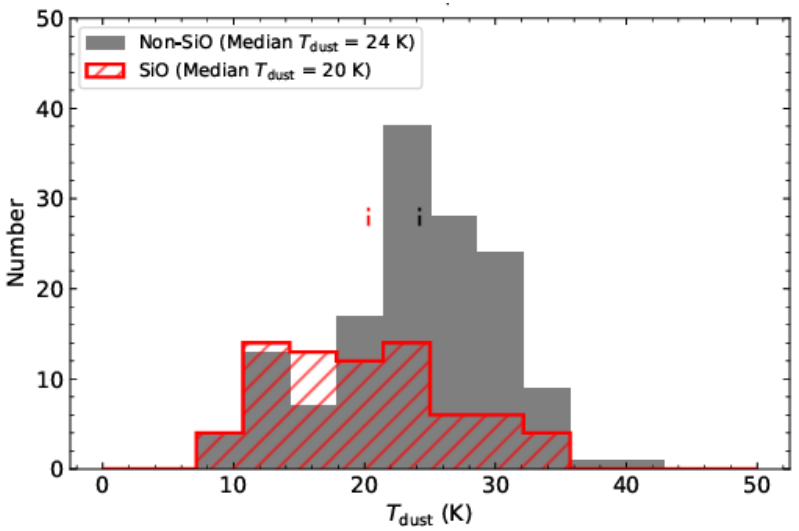


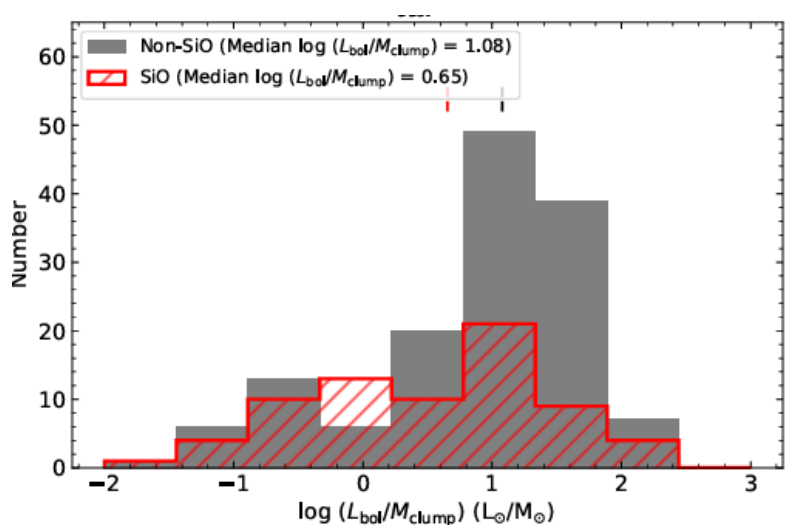

# 議論: 統計

- H2, SiO柱密度と$L_{\rm bol}/M_{\rm clump}$との関係

  SiO柱密度はbeam filling factor~1として計算
  SiO存在度はおよそ$2-3\times10^{-10}$
  $L_{\rm bol}/M_{\rm clump}$, ダスト温度とは無相関

- SiO輝線光度

  同じ$L_{\rm bol}$でもダスト温度が低いほど輝線が強い
  $L_{\rm bol}/M_{\rm clump}$との相関は見られない

  → 気相中のSiO存在度を上昇させる
  メカニズムがあるはず。

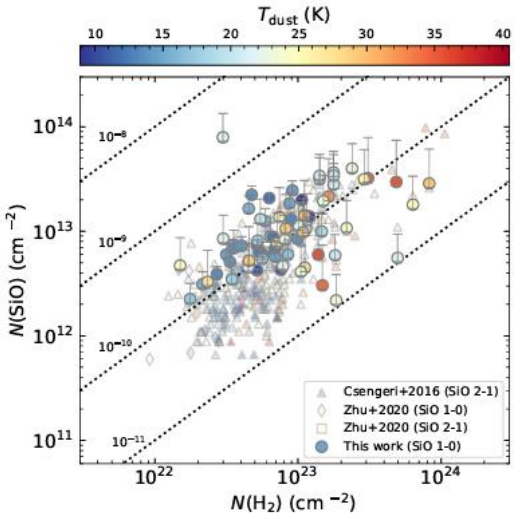


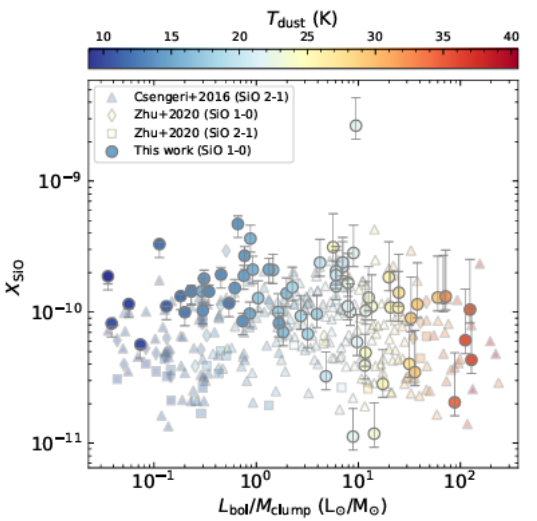


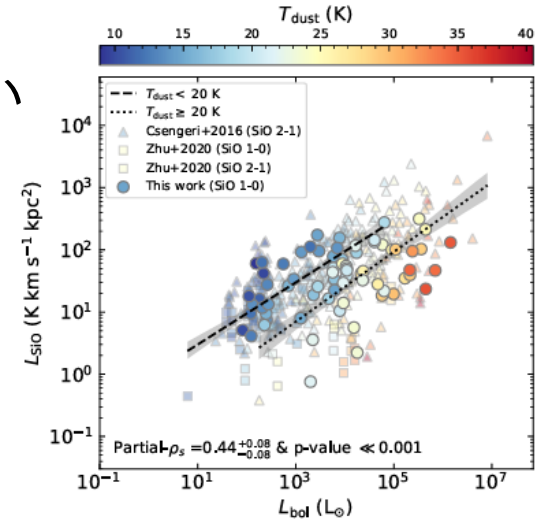


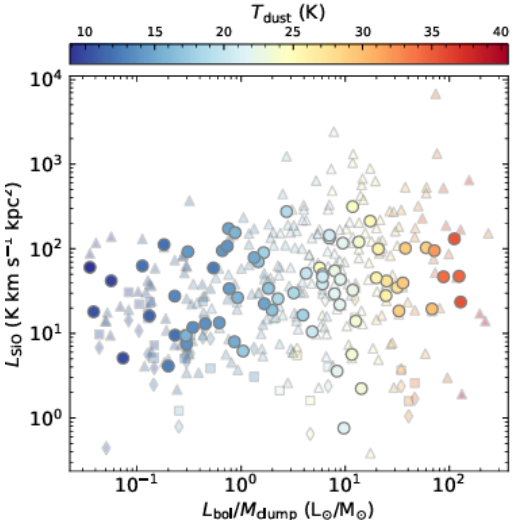


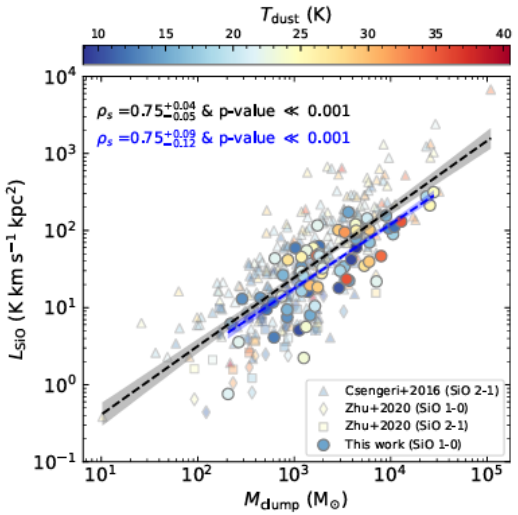


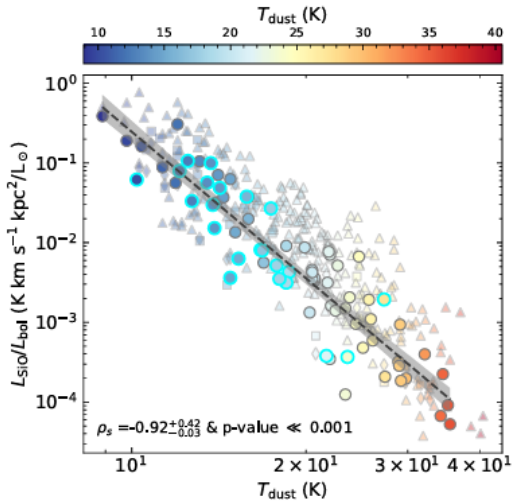


- $L_{\rm SiO}$は$M_{\rm clump}$と相関
- $L_{\rm SiO}/L_{\rm bol}$はダスト温度と負の相関をもつ
  (進化が進んでいないほど$L_{\rm SiO}/L_{\rm bol}$は大きい)

# 議論: SiO輝線のwingの有無

- SiO輝線を元にして各天体を 2 グループに分類
  - non-wing SiO source:
    輝線形状にwingを持たない&線幅が8 km/s以下
    outflowやjetのような星形成活動に起因するSiO放射をもたないサンプルに対応
  - SiO wing source: それ以外

  non-wing天体は進化が進んでおらず、SiO輝線放射が強い
- 考えられる原因
  - 減衰したoutflowによる影響
  - photo-desorption
  - 遅い衝撃波による影響
    (cloud-cloud collision, converging flow, global-infalling, ...)

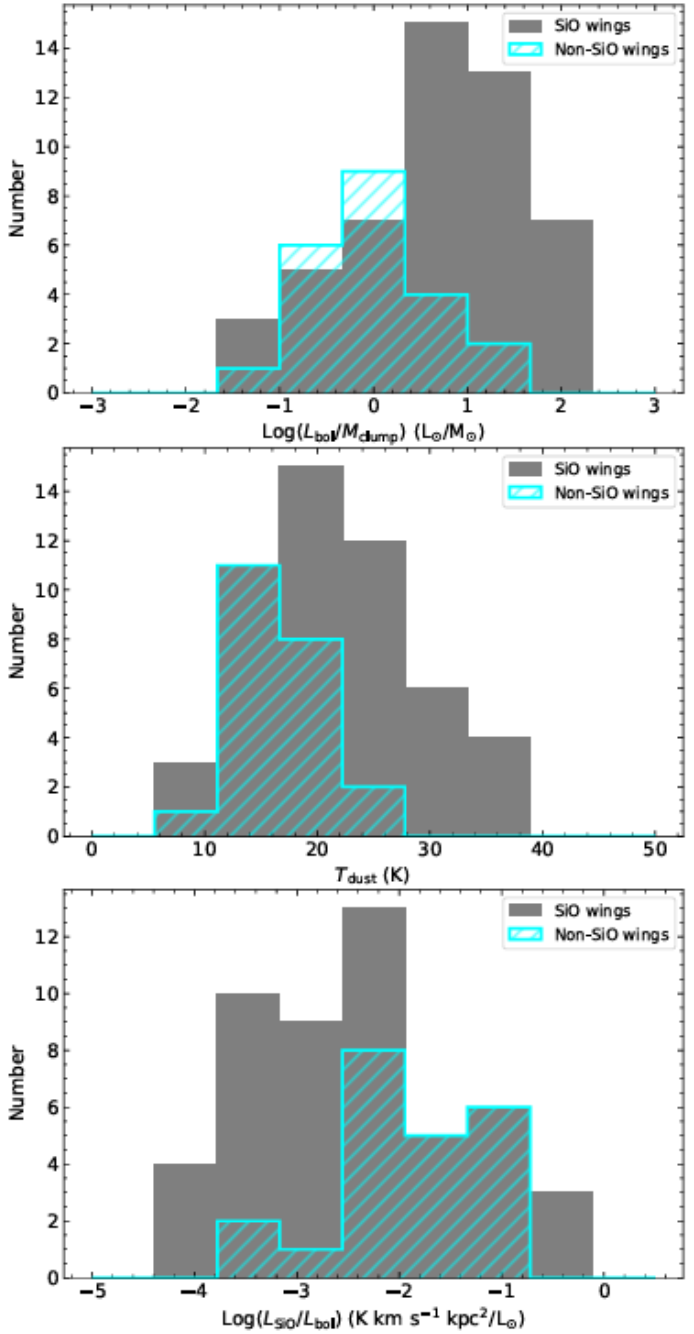

# 議論: 各メーザーとの関係性

- $H_2O$メーザー、$CH_3OH$メーザーとの相関の有無
  - $H_2O$との相関はそこまで強くない。
    $H_2O$はoutflowに付随するためか。
  - $CH_3OH$とは強い正の相関を示す。
    衝撃波や膨張する電離ガスにより$CH_3OH$が励起すると共に、
    SiOもダストからたたき出されたか。

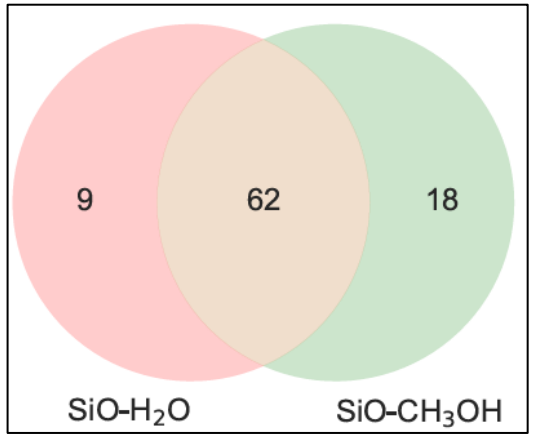


各メーザーの付随状況

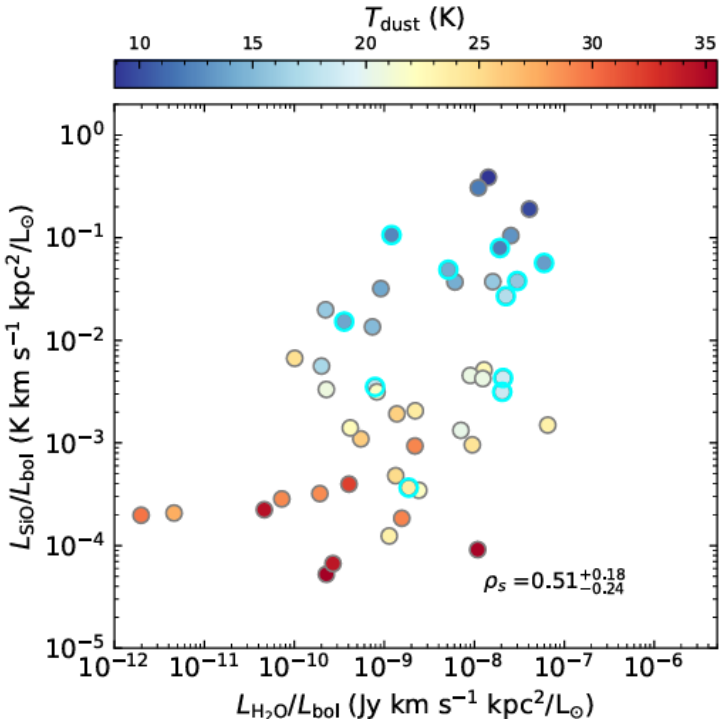


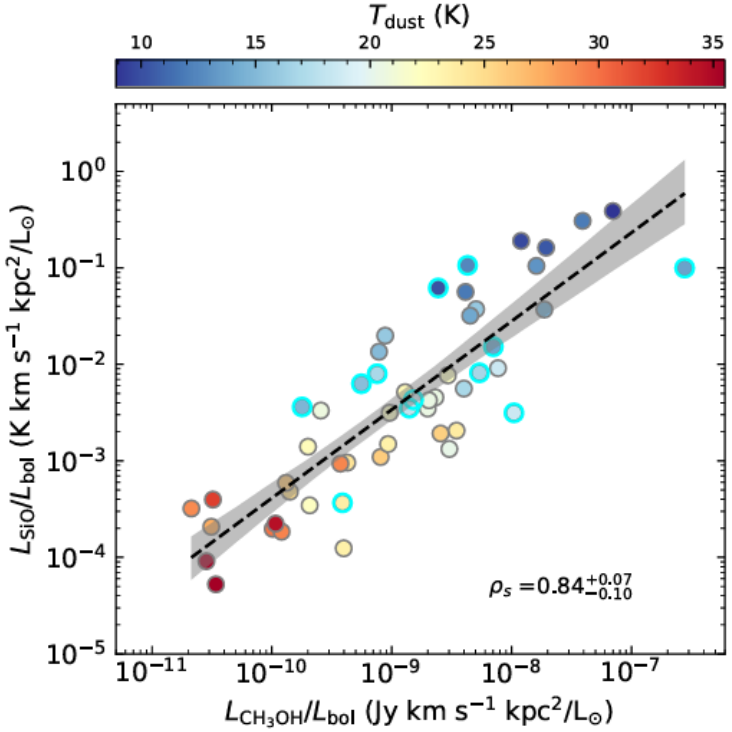

37. **A kinematic study of the disc-outflow system around a high-mass protostar G59.783+0.065 probed by methanol and water masers**

M. Nakamura, K. Motogi, H. Nakamura, Y. Yonekura, K. Fujisawa ★ Class II CH3OH masers are used as a convenient tracer of disc-like structures in high-mass star formation. However, more than half of them show a complex distribution in Very Long Baseline Interferometry (VLBI) maps. The origin of such a complex distribution is still unknown. We conducted VLBI monitoring observations to unveil the origin of a complex class II CH3OH maser in the high-mass star-forming region G59.783+0.065. We observed the CH3OH maser at 6.7 GHz and the H2O maser at 22 GHz to probe detailed circumstellar kinematics and structures by the Japanese VLBI network and the VLBI Exploration of Radio Astrometry. We found similar bipolar distributions in both masers, specifically two clusters located 2000 au apart along the East-West direction. We detected a linear distribution of CH3OH masers in the Western cluster. A position-velocity diagram shows that the Western CH3OH masers trace a rotating disc-wind or infalling component inside an edge-on disc-like structure. In contrast to the simple bipolar expanding motions of the H2O masers, the CH3OH masers exhibited complex motions despite their spatial coincidence. Some of the Eastern CH3OH masers showed bipolar expansions similar to the H2O masers, while others displayed random or even inward motions. Such complex kinematics and their close association with the H2O maser could occur at the boundary between outflow and inflow. We suggest that the complex distribution of class II CH3OH masers, like G59.783+0.065 arises from several distinct circumstellar structures that simultaneously achieve maser excitation.

大質量星形成領域G59.783+0.065について、
複数の期間に跨って$H_2O$及び$CH_3OH$メーザーを観測

- 西側$CH_3OH$メーザーにより、回転円盤と
  思われる構造をトレース
- 東側で検出されるメーザーは
  outflowとinflowの境界付近を反映している可能性

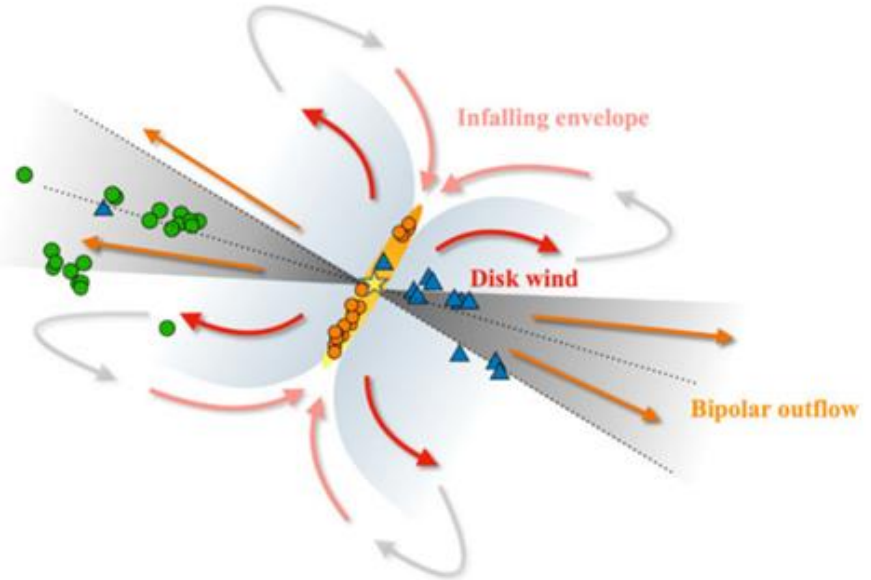

# イントロ・観測

- 大質量星周囲の円盤・エンベロープの構造を理解することは、
  星形成過程の理解にとって重要
- メーザーは、大質量星形成領域の円盤やアウトフローの空間・力学的構造を
  調べるのに有用

    特にClass II $CH_3OH$メーザーは大質量原始星の近傍100-1000AUで励起されるため、原始星の位置や周囲の構造を調べるのによく使われる。

- VLBIにより、複雑な分布をもつ$CH_3OH$メーザーが観測されてきたが、
  その物理的な起源についてはよく分かっていない。

    →複数の期間に渡って$CH_3OH$, $H_2O$メーザーを観測し、
    固有運動を調べることで、メーザーの起源を調べる

- 観測対象: 大質量星形成領域G59.783+0.065
- 観測: VERA($H_2O$メーザー): 2016年2-5月の間に4回
  JVN($CH_3OH$メーザー): 2016年8月-2019年4月の間に6回

# 結果

- $H_2O$メーザー
  2か所で検出。東側の成分はEpoch 4で消滅
- $CH_3OH$メーザー
  東側は$H_2O$メーザー付近に付随
  西側はおよそ直線状に分布
- 複数の観測を元に、”重心”に対する固有運動を推定

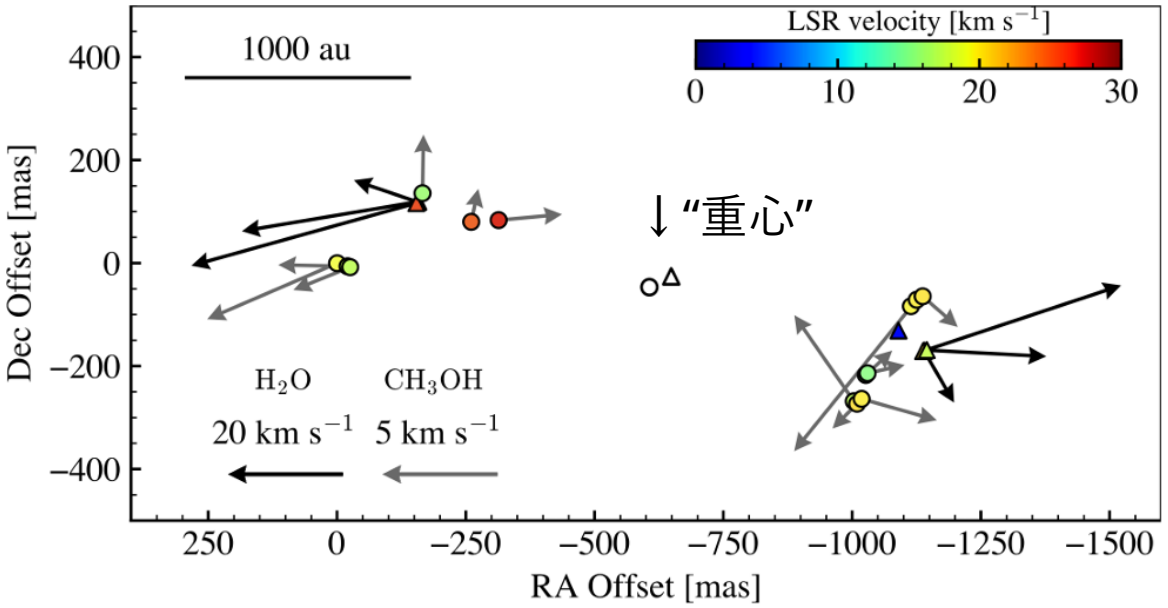


←各成分の固有運動
△: $H_2O$, ○: $CH_3OH$

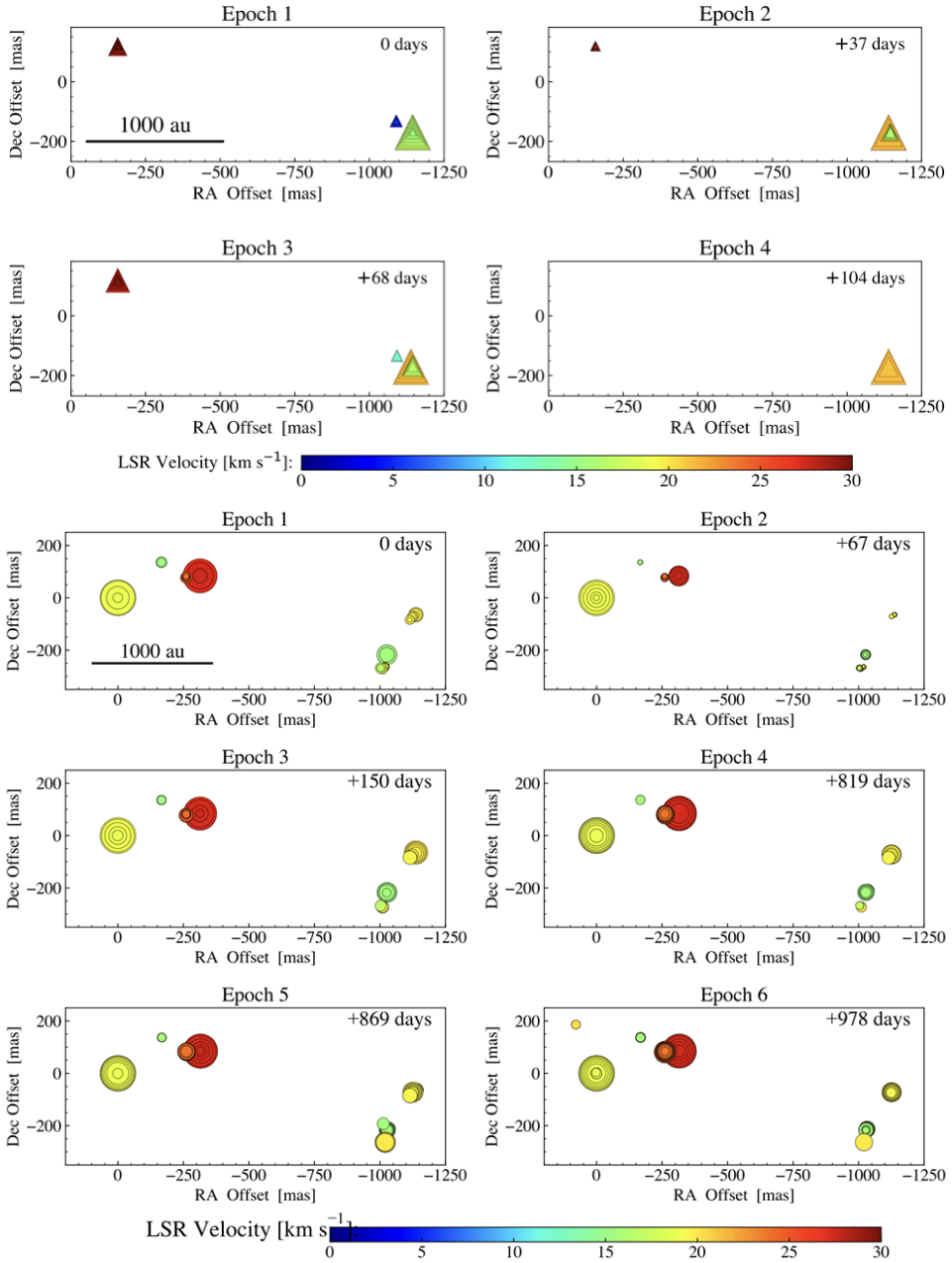


↑ 上: $H_2O$, 下: $CH_3OH$

# 議論: 過去の観測との比較

- $CH_3OH$

  先行の観測と似た位置に分布。
  約15年の間は$CH_3OH$を励起する
  物理構造が定常的に存在。

- $H_2O$

  従来の観測では西側のみ観測。
  episodicな質量放出による
  時間変動を反映？

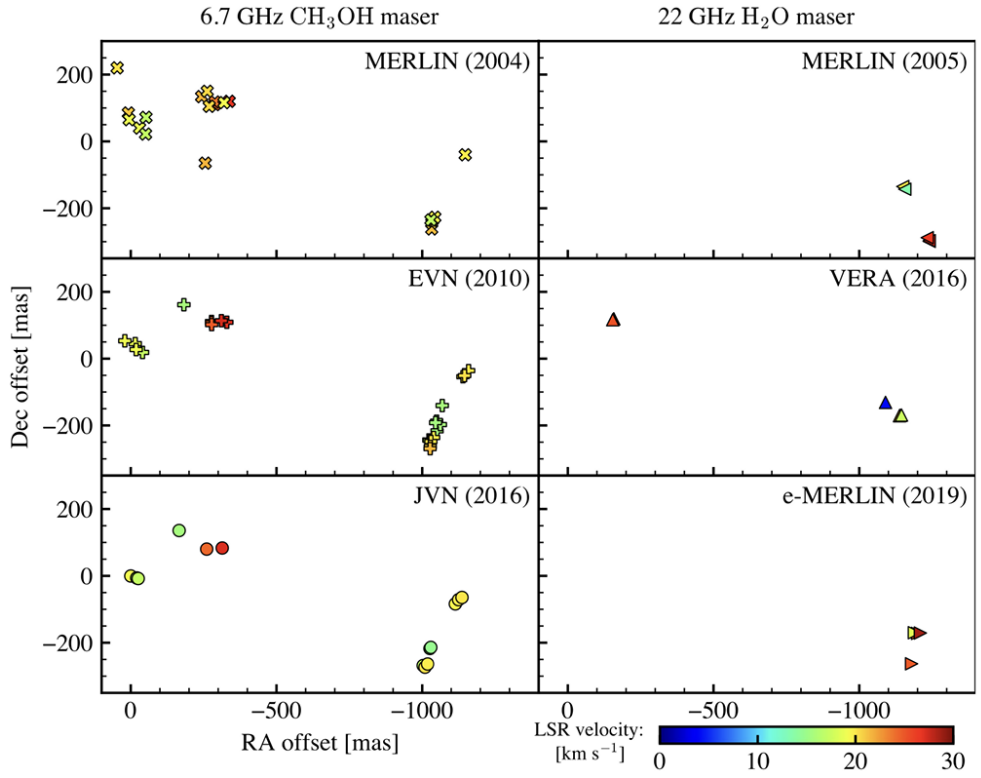


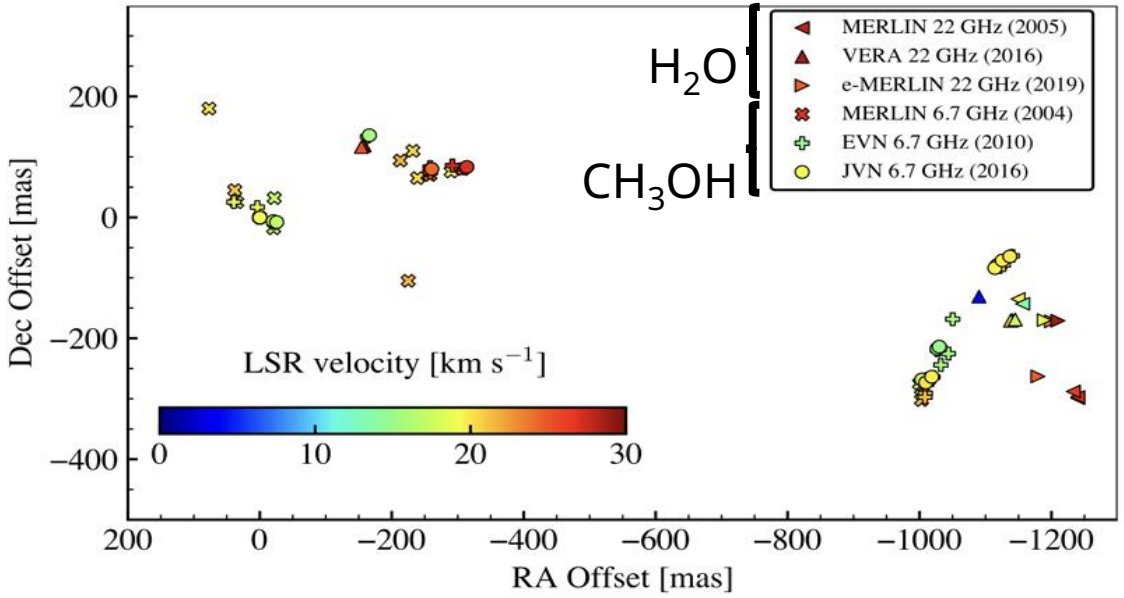

# 議論: 西側の$CH_3OH$成分の解析

- 直線状の$CH_3OH$分布→edge-on disk？

  直線状分布をフィッティング
  →直線状に原始星があると仮定

  直線からのoffsetを取る
  →$CH_3OH$成分は細長い楕円上に分布

- PV図: 楕円の青方側に分布
  →降着or拡大する回転構造を反映

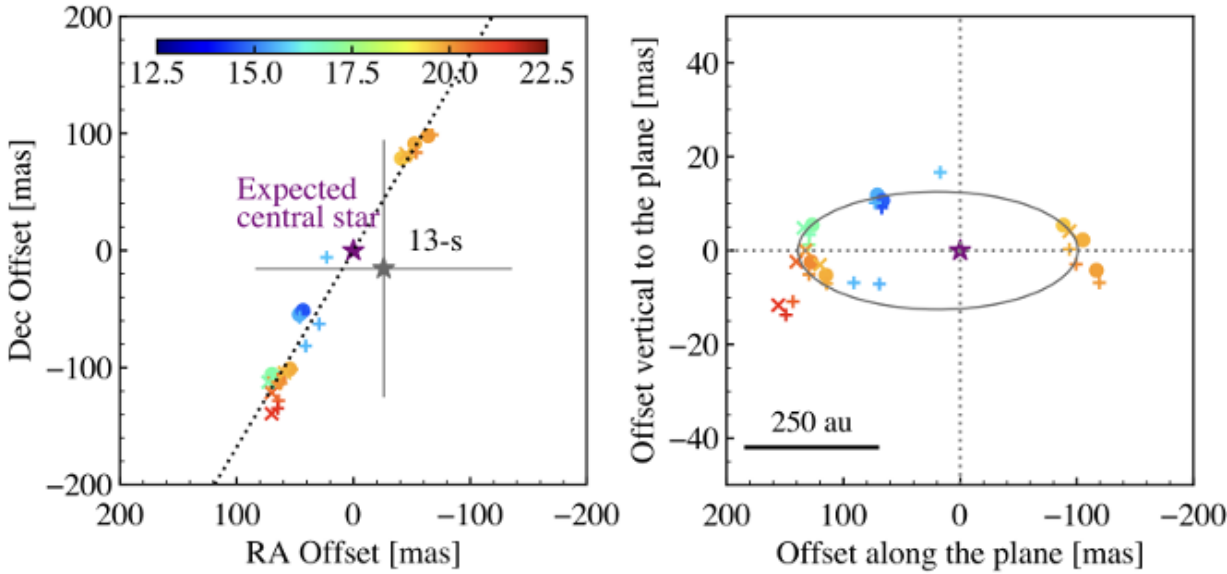


13-s: millimetre continuum peak

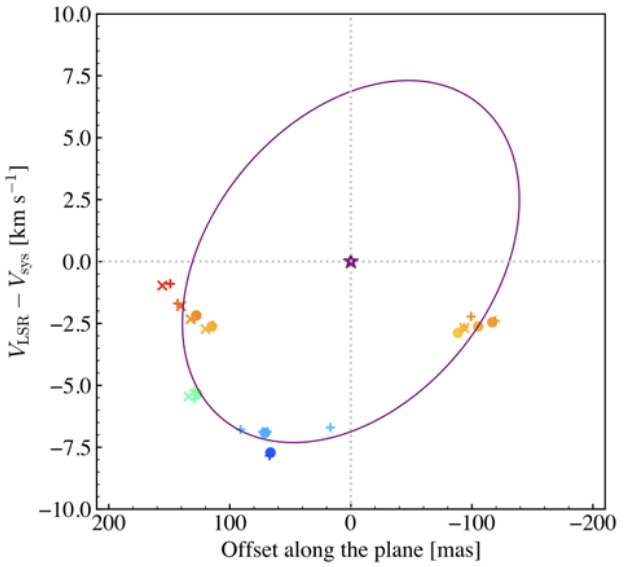


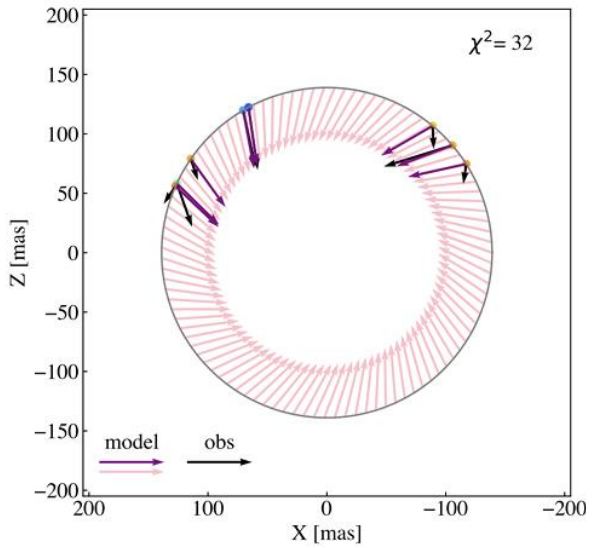


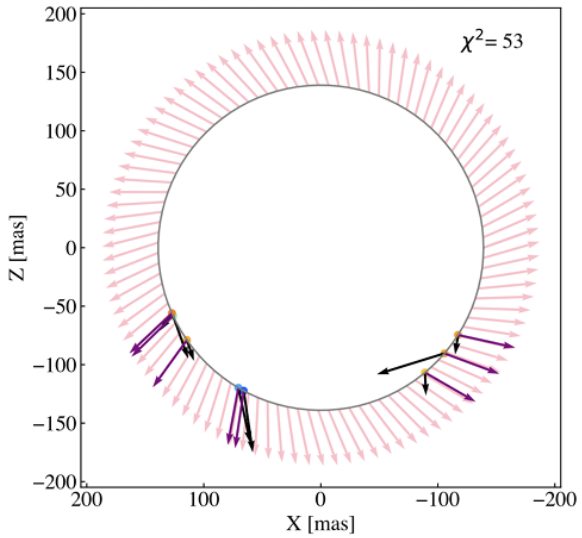


- 固有運動とも比較

降着&回転の方が適しているように思われる

- 楕円の外の成分
  - リングの厚み？
  - 渦状腕の一部？

# 議論: 東側の$CH_3OH$, $H_2O$成分の解釈

- 分子毎の位置・速度構造に違い

$H_2O$:　高速度成分。
　　原始星から離れる方向

$CH_3OH$: 比較的低速度。
　　方向はバラバラ。
　　$H_2O$とは反対方向の成分も。

- $CH_3OH$はoutflowとinflowの境界付近をトレースしている？
- 以上の結果をまとめると右図のような描像になる

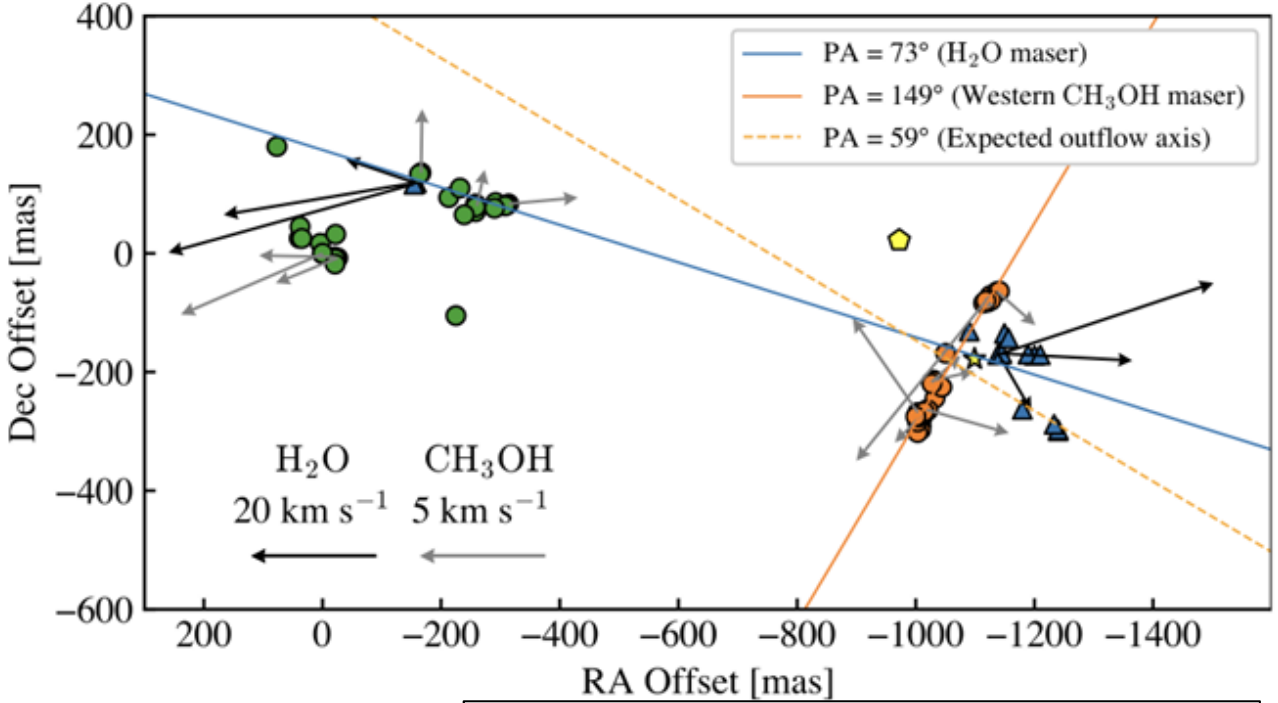


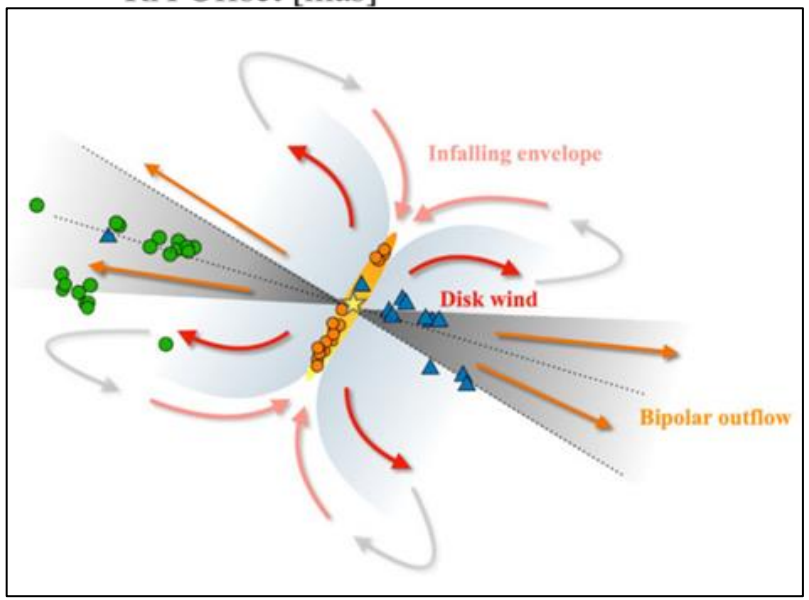

32. **A low-mass line-rich core found in Massive Star-forming Region IRAS 16351-4722**

**Meizhu Liu, Sheng-Li Qin, Tie Liu, Mengyao Tang, Sheng-Yuan Liu, Li Chen, ChuanShou Li, HongQiong Shi, Xiaohu Li, Tianwei Zhang, Ken'ichi Tatematsu, Fengwei Xu, Yuefang Wu** ★ We present ALMA sub-arcsecond-resolution observations of both continuum and molecular lines at 345 GHz towards the massive star-forming region IRAS 16351-4722 (hereafter I16351). A total of 12 dust cores were detected based on high spatial resolution observations of the continuum. Among them, a high-mass core (11.6 Msun) and a low-mass core (1.7 Msun) show abundant molecular line emissions. 164 molecular transitions from 29 species and 104 molecular transitions from 25 species are identified in the high-mass and low-mass cores, respectively. Complex organic molecules (COMs) such as CH3OH, CH3OCHO, CH3OCH3, C2H5OH, and C2H5CN are detected in the two cores. Under the assumption of local thermodynamic equilibrium (LTE), rotational temperatures and column densities of the COMs are derived with the XCLASS software. The maximum rotation temperature values in the low-mass core and the high-mass core were found to be approximately 130 K and 198 K, respectively. Additionally, the line widths in the high-mass core are larger than those in the low-mass one. Abundant complex organic molecular line transitions, high gas temperatures, and smaller line widths indicate the presence of a low-mass line-rich core in the massive star formation region for the first time, while the high-mass line-rich core shows hot core property. When comparing the molecular abundances of CH3OH, CH3OCHO, CH3OCH3 and C2H5OH of the two cores with other hot cores and hot corinos reported in the literature, we further confirm that both a hot core and a low-mass line-rich core are simultaneously detected in I16351.

I16351のhot coreとその周辺のlow-mass coreを観測

- 大質量星形成領域で初めてlow-mass line-rich coreを検出

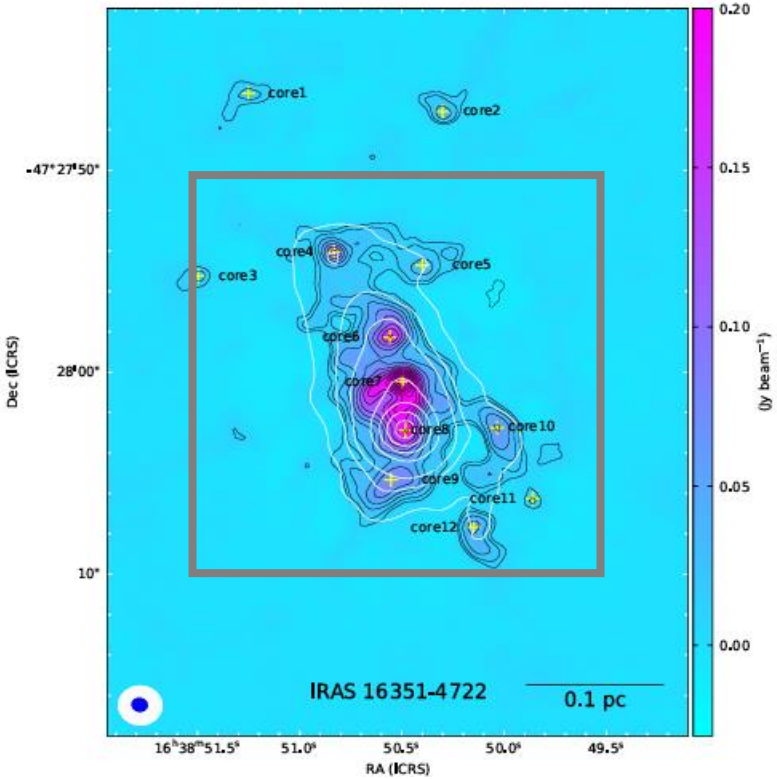


ALMA Band 7

← 870 μm (color & black contours)
3 mm (white contours)

→

870 μm (color)
each molecule (black contours)

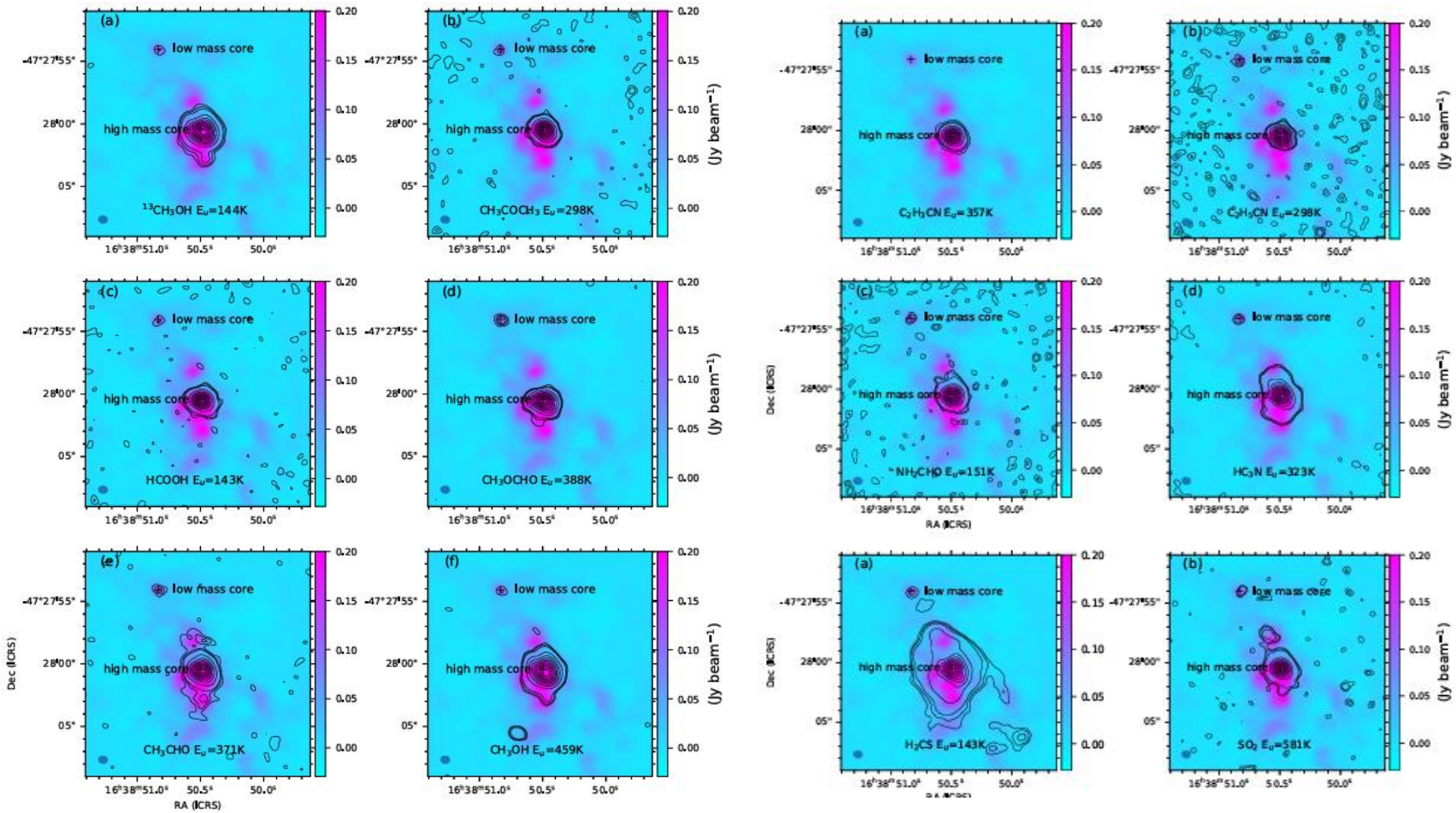

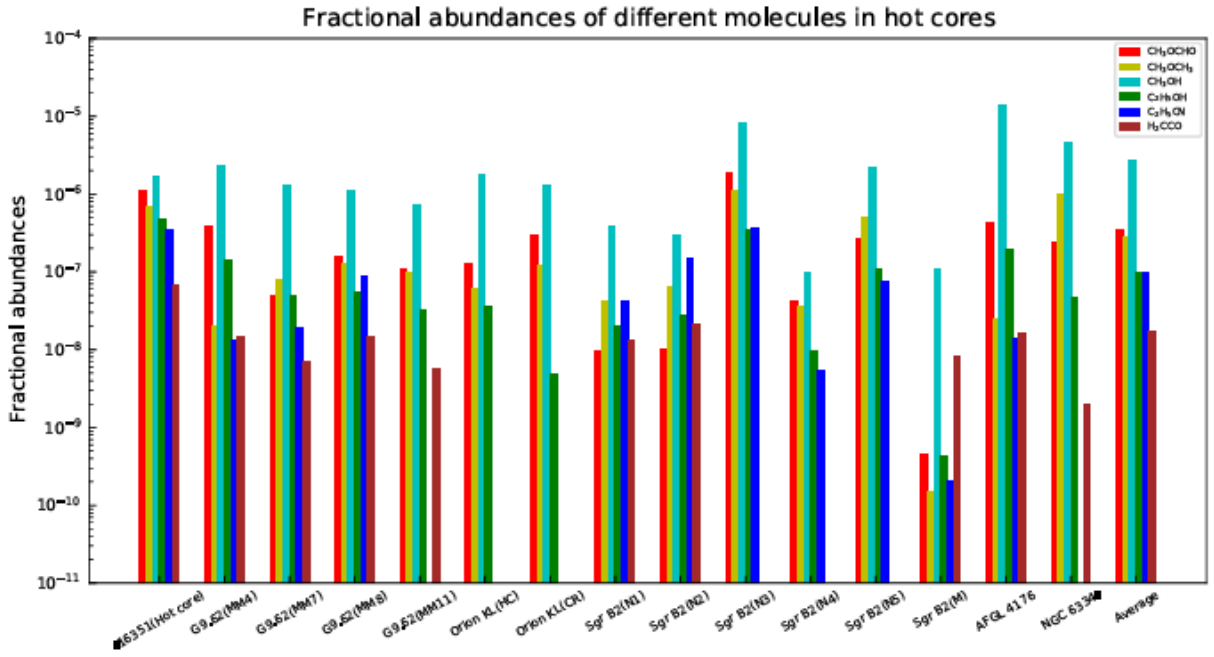


# 他のhot core, hot corinoとの比較

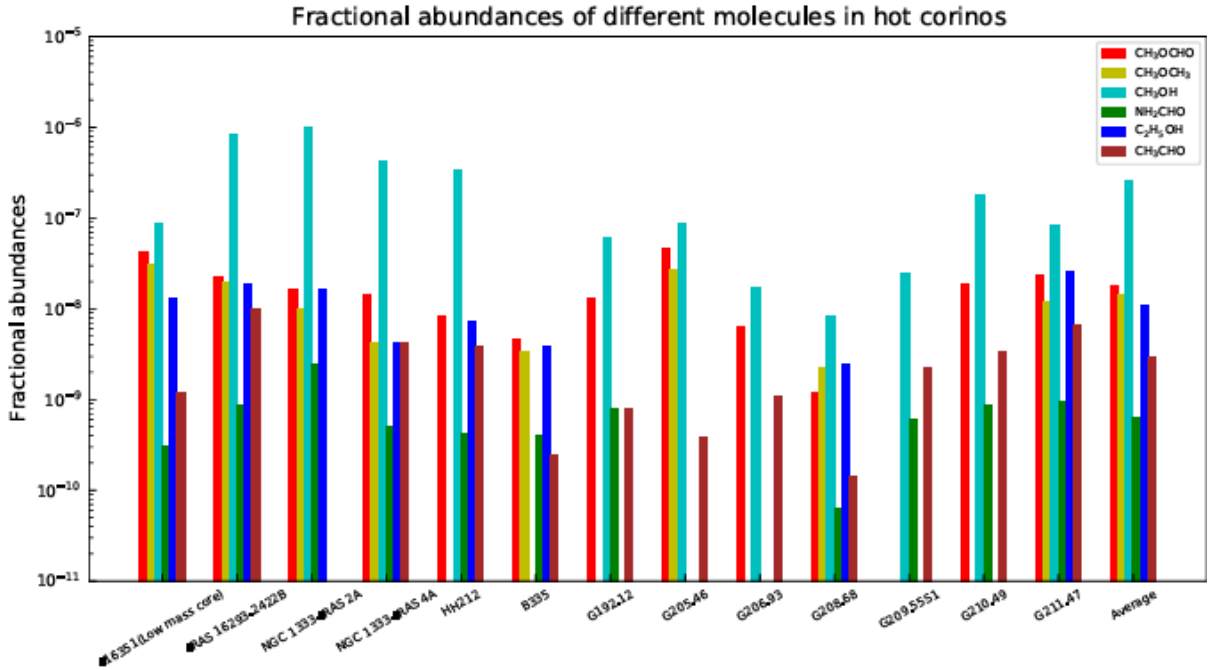


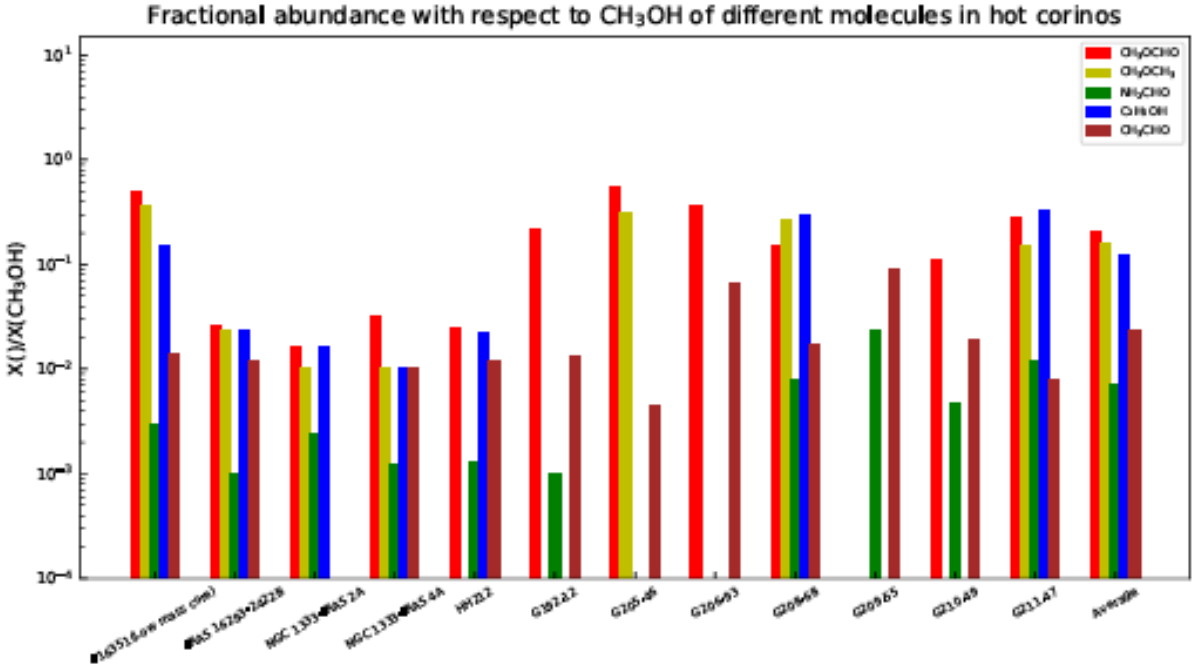

38. **Early Planet Formation in Embedded Disks (eDisk) X: Compact Disks, Extended Infall, and a Fossil Outburst in the Class I Oph IRS43 Binary**

**Suchitra Narayanan, Jonathan P. Williams, John J. Tobin, Jes K. Jorgensen, Nagayoshi Ohashi, Zhe-Yu Daniel Lin, Merel L. R. van't Hoff, Zhi-Yun Li, Adele L. Plunkett, Leslie W. Looney, Shigehisa Takakuwa, Hsi-Wei Yen, Yusuke Aso, Christian Flores, Jeong-Eun Lee, Shih-Ping Lai, Woojin Kwon, Itziar de Gregorio-Monsalvo, Rajeeb Sharma, Chang Won Lee** ★ We present the first results from the Early Planet Formation in Embedded Disks (eDisk) ALMA Large Program toward Oph IRS43, a binary system of solar mass protostars. The 1.3 mm dust continuum observations resolve a compact disk, 6au radius, around the northern component and show that the disk around the southern component is even smaller, $<$ 3 au. CO, 13CO, and C18O maps reveal a large cavity in a low mass envelope that shows kinematic signatures of rotation and infall extending out to 2000au. An expanding CO bubble centered on the extrapolated location of the source 130 years ago suggests a recent outburst. Despite the small size of the disks, the overall picture is of a remarkably large and dynamically active region.

eDisk論文

Oph IRS43の連星の円盤を観測

# 1.3 continuum image

| Source | ICRS R.A. [h m s] | ICRS Dec. [d m s] | Deconvolved FWHM, PA [mas,°] | Peak $I_\nu, T_b$ [mJy beam$^{-1}$, K] | $F_\nu$ [mJy] | incl [°] | Dust Mass [$M_\oplus$] |
|---|---|---|---|---|---|---|---|
| VLA1 | 16:27:26.906 | −24:40:50.81 | 89×18, 133.5 ± 1.1 | 3.30, 62 | 10.62 | 78 | 3.4 |
| VLA2 | 16:27:26.911 | −24:40:51.40 | 19×16, 62.5 ± 6.3 | 0.88, 20 | 1.08 | 32 | 0.34 |

円盤半径
VLA1: ~ 6 AU, VLA2: ≲ 3 AU

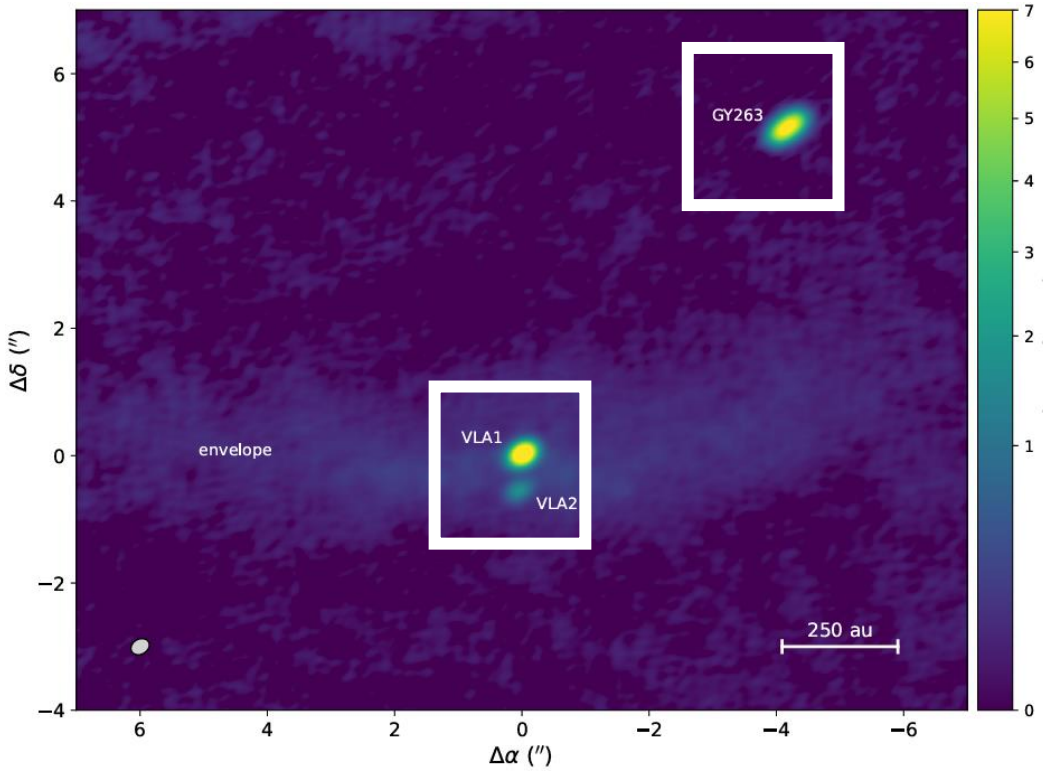


GY263: 遷移円盤

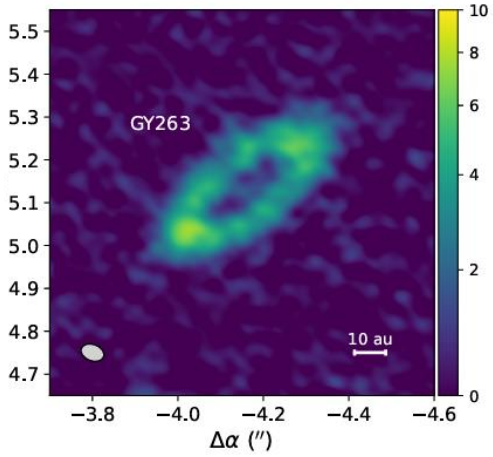


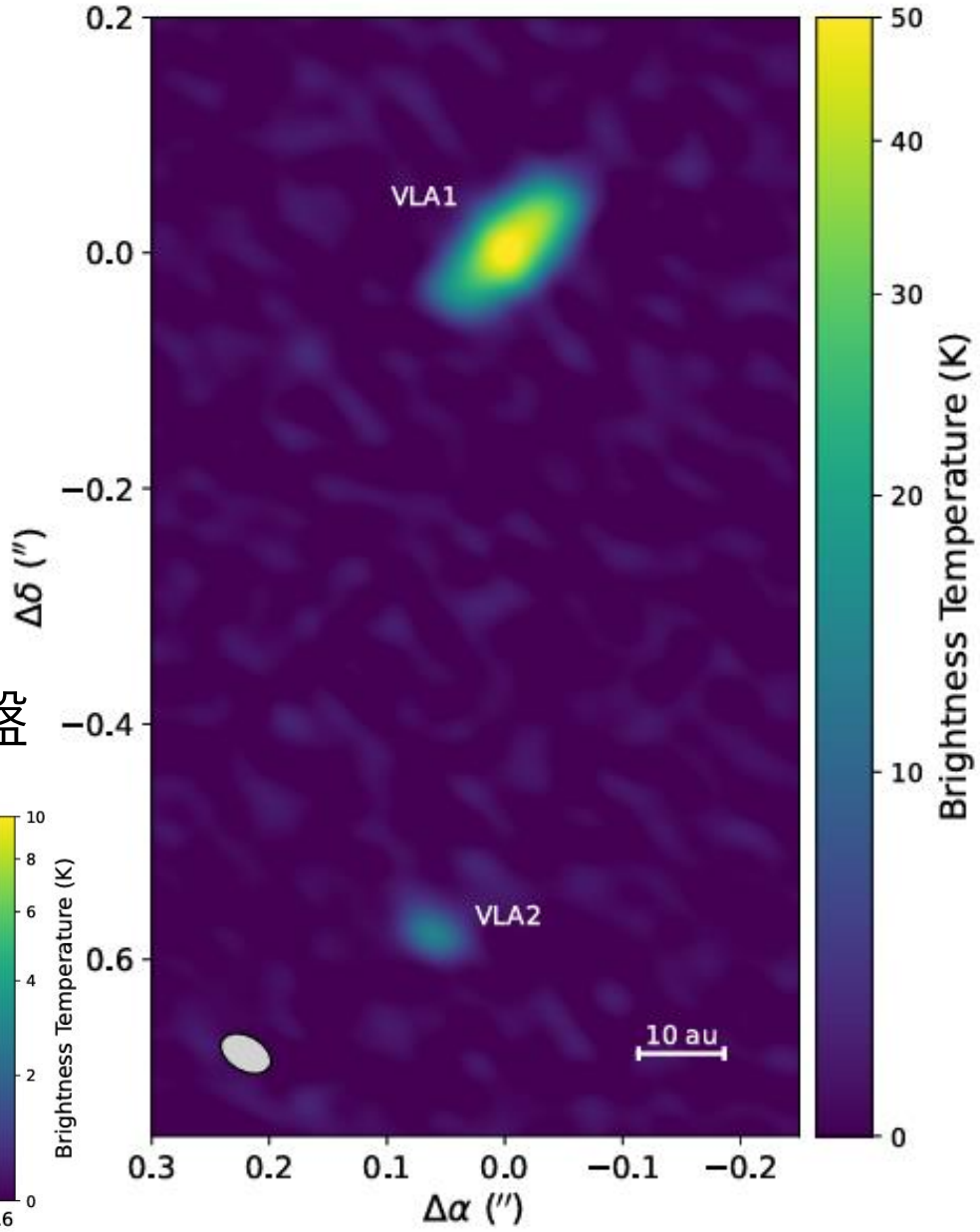

CO, $^{13}$CO, C$^{18}$O, $H_2CO$, SO

<u>PV図:</u>
ケプラー回転より速い運動
→回転&降着を示す
SOは円盤への降着によるshockをトレース？

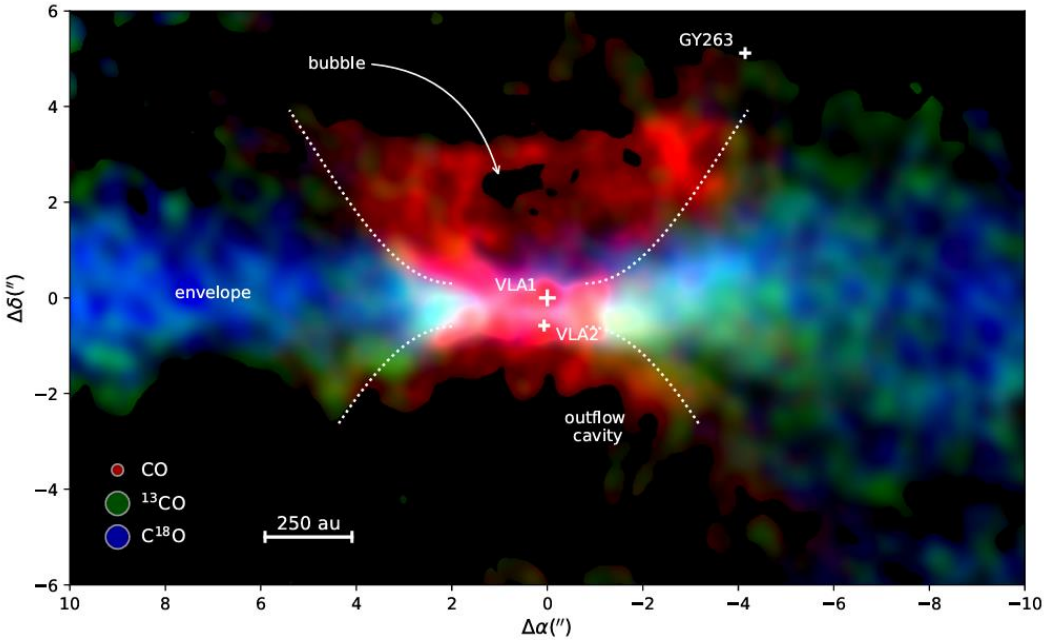


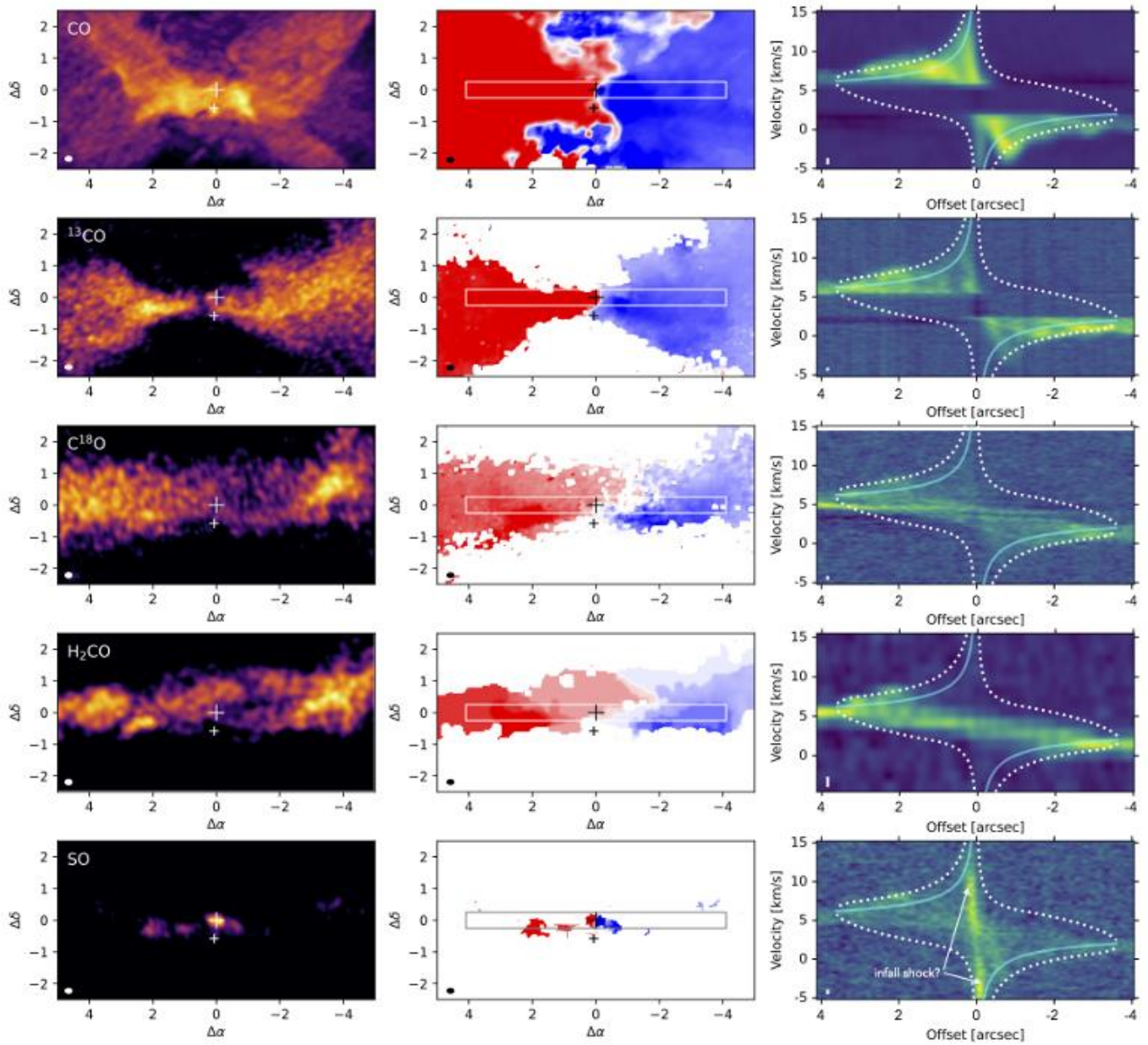

# CO channel maps
# CO ring: 約130年前のoutburstか

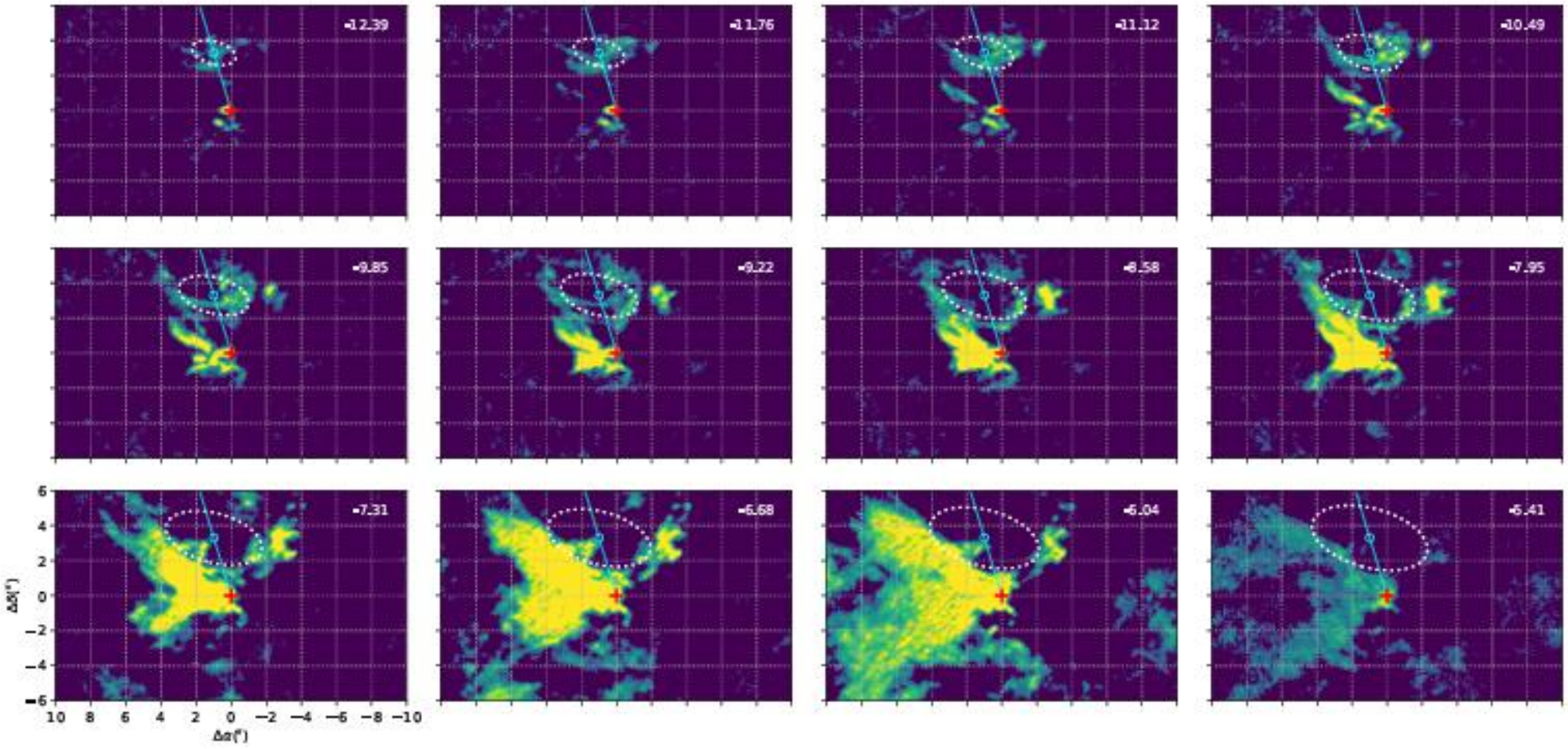

## 28. Hydrocarbon chemistry in inner regions of planet forming disks

**Jayatee Kanwar, Inga Kamp, Peter Woitke, Christian Rab, Wing-Fai Thi, Michiel Min** ★ The analysis of the mid-infrared spectra helps understanding the composition of the gas in the inner, dense and warm terrestrial planet forming region of disks around young stars. ALMA has detected hydrocarbons in the outer regions of the planet forming disk and Spitzer detected C2H2 in the inner regions. JWST- MIRI provides high spectral resolution observations of C2H2 and a suite of more complex hydrocarbons are now reported. Interpreting the fluxes observed in the spectra is challenging and radiation thermo-chemical codes are needed to properly take into account the disk structure, radiative transfer, chemistry and thermal balance. Various disk physical parameters like the gas-to-dust ratio, dust evolution including radial drift, dust growth and settling can affect the fluxes observed in the mid-IR. Still, thermo-chemical disk models were not always successful in matching all observed molecular emission bands simultaneously. The goal of this project is two-fold. We analyse the warm carbon chemistry in the inner regions of the disk, i.e. within 10 au to find pathways forming C2H2 potentially missing from the existing chemical networks. Second, we analyse the effect of the new chemistry on the line fluxes of acetylene. We use radiative thermo-chemical disk code PRODIMO to expand the hydrocarbon chemistry that occurs in a typical standard T Tauri disks. We used the UMIST and the KIDA rate databases for collecting reactions for the species. We include a number of three-body and thermal decomposition reactions from STAND2020 network. We included isotopomers for the species that were present in the databases. The chemistry is then analysed in the regions that produce observable features in the mid-infrared spectra. The effect of expanding the hydrocarbon chemistry on the mid-infrared spectra is studied.

## 30. 3D structure of HII regions in the star-forming complex S254-S258

**Maria S. Kirsanova, Alexei V. Moiseev, Paul A. Boley** ★ The S254-258 star-forming complex is a place of massive star formation where five OB-stars have created HII regions, visible as optical nebulae, and disrupted the parental molecular gas. In this work, we study the 3D structure of these HII regions using optical spectroscopy and tunable-filter photometry with the 6-m and 1-m telescopes of the Special Astrophysical Observatory of the Russian Academy of Sciences. We construct maps of the optical extinction, and find that the HII emission is attenuated by neutral material with $2 \leq A_V \leq 5$ mag. The typical electron density in S255, and S257 is $\approx 100$ cm$^{-3}$, with enhancements up to 200 cm$^{-3}$ in their borders, and up to 400 cm$^{-3}$ toward the dense molecular cloud between them, where active star formation is taking place. We show that either a model of a clumpy dense neutral shell, where UV photons penetrate through and ionize the gas, or a stellar wind, can explain the shell-like structure of the ionized gas. S255 is surrounded by neutral material from all sides, but S257 is situated on the border of a molecular cloud and does not have dense front and rear walls. The compact HII regions S256 and S258 are deeply embedded in the molecular clouds.

31. ## 3D Global Simulations of Accretion onto Gap-opening Planets: Implications for Circumplanetary Disc Structures and Accretion Rates

**Ya-Ping Li, Yi-Xian Chen, Douglas N. C. Lin** ★ We perform a series of 3D simulations to study the accretion of giant planet embedded in protoplanetary discs (PPDs) over gap-opening timescales. We find that the accretion mass flux mainly comes from the intermediate latitude above the disc midplane. The circumplanetary disc (CPD) for a super-thermal planet is rotation-supported up to ∼20-30% of the planet Hill radius. While both mass inflow and outflow exists in the CPD midplane, the overall trend is an outflow that forms a meridional circulation with high-latitude inflows. We confirm the absence of accretion outburst from disc eccentricity excited by massive planets in our 3D simulations, contrary to the consensus of previous 2D simulations. This suggests the necessity of 3D simulations of accretion even for super-Jupiters. The accretion rates of planets measured in steady-state can be decomposed into the "geometric" and "density depletion" factors. Through extensive parameter survey, we identify a power-law scaling for the geometric factor $\propto q_{\rm th}^{2/3}$ for super-thermal planets ($q_{\rm th}$ being the thermal mass ratio), which transforms to $\propto q_{\rm th}^{2}$ for less massive cases. The density depletion factor is limited by the disc accretion rate for mildly super-thermal planets, and by gap-opening for highly super-thermal ones. Moderate planetary eccentricities can enhance the accretion rates by a factor of $2-3$ through making the gap shallower, but does not impact the flow geometry. We have applied our simulations results to accreting protoplanet system PDS 70 and can satisfactorily explain the accretion rate and CPD size in observations.

## 33. A JWST survey of the Trapezium Cluster & inner Orion Nebula. I. Observations & overview

**M. J. McCaughrean, S. G. Pearson** ★ We present a near-IR survey of the Trapezium Cluster and inner Orion Nebula using the NASA/ESA/CSA James Webb Space Telescope. The survey with the NIRCam instrument covers 10.9 x 7.5 arcminutes ( 1.25 x 0.85 pc) in twelve wide-, medium-, and narrow-band filters from 1-5 microns and is diffraction-limited at all wavelengths, providing a maximum spatial resolution of 0.063 arcsec at 2 microns, corresponding to 25 au at Orion. The suite of filters chosen was designed to address a number of scientific questions including the form of the extreme low-mass end of the IMF into the planetary-mass range to 1 Jupiter mass and below; the nature of ionised and non-ionised circumstellar disks and associated proplyds in the near-IR with a similar resolution to prior HST studies; to examine the large fragmented outflow from the embedded BN-KL region at very high resolution and fidelity; and to search for new jets and outflows from young stars in the Trapezium Cluster and the Orion Molecular Cloud 1 behind. In this paper, we present a description of the design of the observational programme, explaining the rationale for the filter set chosen and the telescope and detector modes used to make the survey; the reduction of the data using the JWST pipeline and other tools; the creation of large colour mosaics covering the region; and an overview of the discoveries made in the colour images and in the individual filter mosaics. Highlights include the discovery of large numbers of free-floating planetary-mass candidates as low as 0.6 Jupiter masses, a significant fraction of which are in wide binaries; new emission phenomena associated with the explosive outflow from the BN-KL region; and a mysterious "dark absorber" associated with a number of disparate features in the region, but which is seen exclusively in the F115W filter. Further papers will examine those discoveries and others in more detail.

## 34. Early phases of star formation: testing chemical tools

**N. C. Martinez, S. Paron** ★ The star forming processes strongly influence the ISM chemistry. Nowadays, there are available many high-quality databases at millimeter wavelengths. Using them, it is possible to carry out studies that review and deepen previous results. If these studies involve large samples of sources, it is preferred to use direct tools to study the molecular gas. With the aim of testing these tools such as the use of the HCN/HNC ratio as a thermometer, and the use of $H^{13}CO^+$, $HC_3N$, $N_2H^+$, and $C_2H$ as "chemical clocks", we present a molecular line study towards 55 sources representing massive young stellar objects (MYSOs) at different evolutive stages: infrared dark clouds (IRDCs), high-mass protostellar objects (HMPOs), hot molecular cores (HMCs) and ultracompact HII regions (UCHII). We found that the use of HCN/HNC ratio as an universal thermometer in the ISM should be taken with care because the HCN optical depth is a big issue that can affect the method. Hence, this tool should be used only after a careful analysis of the HCN spectrum, checking that no line, neither the main nor the hyperfine ones, present absorption features. We point out that the analysis of the emission of $H^{13}CO^+$, $HC_3N$, $N_2H^+$, and $C_2H$ could be useful to trace and distinguish regions among IRDCs, HMPOs and HMCs. The molecular line widths of these four species increase from the IRDC to the HMC stage, which can be a consequence of the gas dynamics related to the star-forming processes taking place in the molecular clumps. Our results do not only contribute with more statistics regarding to probe such chemical tools, useful to obtain information in large samples of sources, but also complement previous works through the analysis on other types of sources.

## 35. An improved dynamical Poisson equation solver for self-gravity

**Ryunosuke Maeda, Tsuyoshi Inoue, Shu-ichiro Inutsuka** ★ Since self-gravity is crucial in the structure formation of the universe, many hydrodynamics simulations with the effect of self-gravity have been conducted. The multigrid method is widely used as a solver for the Poisson equation of the self-gravity; however, the parallelization efficiency of the multigrid method becomes worse when we use a massively parallel computer, and it becomes inefficient with more than $10^4$ cores, even for highly tuned codes. To perform large-scale parallel simulations ($> 10^4$ cores), developing a new gravity solver with good parallelization efficiency is beneficial. In this article, we develop a new self-gravity solver using the telegraph equation with a damping coefficient, $\kappa$. Parallelization is much easier than the case of the elliptic Poisson equation since the telegraph equation is a hyperbolic partial differential equation. We analyze convergence tests of our telegraph equations solver and determine that the best non-dimensional damping coefficient of the telegraph equations is $\tilde{\kappa} \simeq 2.5$. We also show that our method can maintain high parallelization efficiency even for massively parallel computations due to the hyperbolic nature of the telegraphic equation by weak-scaling tests. If the time step of the calculation is determined by heating/cooling or chemical reactions, rather than the CFL condition, our method may provide the method for calculating self-gravity faster than other previously known methods such as the fast Fourier transform and multigrid iteration solvers because gravitational phase velocity determined by the CFL condition using these timescales is much larger than the fluid velocity plus sound speed.

## 36. Co-Evolution of Stars and Gas: Using Analysis of Synthetic Observations to Investigate the Star-Gas Correlation in STARFORGE

**Samuel Millstone, Robert Gutermuth, Stella S. R. Offner, Riwaj Pokhrel, Michael Y. Grudić** ★
We explore the relationship between stellar surface density and gas surface density (the star-gas or S-G correlation) in a 20,000 $M_\odot$ simulation from the STAR FORmation in Gaseous Environments (STARFORGE) Project. We create synthetic observations based on the Spitzer and Herschel telescopes by modeling active galactic nuclei contamination, smoothing based on angular resolution, cropping the field-of-view, and removing close neighbors and low-mass sources. We extract star-gas properties such as the dense gas mass fraction, the Class II:I ratio, and the S-G correlation ($\Sigma_{\rm YSO}/\Sigma_{\rm gas}$) from the simulation and compare them to observations of giant molecular clouds, young clusters, and star-forming regions, as well as to analytical models. We find that the simulation reproduces trends in the counts of young stellar objects and the median slope of the S-G correlation. This implies that the S-G correlation is not simply the result of observational biases but is in fact a real effect. However, other statistics, such as the Class II:I ratio and dense gas mass fraction, do not always match observed equivalents in nearby clouds. This motivates further observations covering the full simulation age range and more realistic modeling of cloud formation.

39. # Variations of the HCO+, HCN, HNC, $N_2H^+$ and $NH_3$ deuterium fractionation in high-mass star-forming regions

**A. G. Pazukhin, I. I. Zinchenko, E. A. Trofimova, C. Henkel, D. A. Semenov** ★ We use spectra and maps of the $J = 1 - 0$ and $J = 2 - 1$ $DCO^+$, DCN, DNC, $N_2D^+$ lines and $1_{11} - 1_{01}$ ortho- and para-$NH_2D$ lines, obtained with the IRAM-30m telescope, as well as observations of their hydrogenated isotopologues to study deuteration processes in five high-mass star-forming regions. The temperature was estimated from $CH_3CCH$ lines, also observed with the IRAM-30m telescope, and from $NH_3$ lines, observed with the 100-m radio telescope in Effelsberg, as well as using the integrated intensity ratios of the $J = 1 - 0$ $H^{13}CN$ and $HN^{13}C$ lines and their main isotopologues. Applying a non-LTE radiative transfer model with RADEX, the gas density and the molecular column densities were estimated. D/H ratios are $0.001 - 0.05$ for $DCO^+$, $0.001 - 0.02$ for DCN, $0.001 - 0.05$ for DNC and $0.02 - 0.4$ for $NH_2D$. The D/H ratios decrease with increasing temperature in the range of $20 - 40$ K and slightly vary at densities $n(H_2) \sim 10^4 - 10^6$ cm$^{-3}$. The deuterium fraction of $N_2H^+$ is $0.008 - 0.1$ at temperatures in the range of $20 - 25$ K and at a density of $\sim 10^5$ cm$^{-3}$. We also estimate relative abundances and find $\sim 10^{-11} - 10^{-9}$ for $DCO^+$ and DNC, $\sim 10^{-11} - 10^{-10}$ for $N_2D^+$ and $\sim 10^{-10} - 10^{-8}$ for $NH_2D$. The relative abundances of these species decrease with increasing temperature. However, the $DCN/H_2$ ratio is almost constant ($\sim 10^{-10}$). The observational results agree with the predictions of chemical models (although in some cases there are significant differences).

## 40. Jupiter Mass Binary Objects in the Trapezium Cluster

**Samuel G Pearson, Mark J McCaughrean** ★ A key outstanding question in star and planet formation is how far the initial mass function of stars and sub-stellar objects extends, and whether or not there is a cut-off at the very lowest masses. Isolated objects in the planetary-mass domain below 13 Jupiter masses, where not even deuterium can fuse, are very challenging to observe as these objects are inherently faint. Nearby star-forming regions provide the best opportunity to search for them though: while they are young, they are still relatively warm and luminous at infrared wavelengths. Previous surveys have discovered a handful of such sources down to 3–5 Jupiter masses, around the minimum mass limit established for formation via the fragmentation of molecular clouds, but does the mass function extend further? In a new James Webb Space Telescope near-infrared survey of the inner Orion Nebula and Trapezium Cluster, we have discovered and characterised a sample of 540 planetary-mass candidates with masses down to 0.6 Jupiter masses, demonstrating that there is indeed no sharp cut-off in the mass function. Furthermore, we find that 9% of the planetary-mass objects are in wide binaries, a result that is highly unexpected and which challenges current theories of both star and planet formation.